Emergence of a Metallic Quantum Solid Phase in a Rydberg-Dressed Fermi Gas

Wei-Han Li,[1] Tzu-Chi Hsieh,[1,*] Chung-Yu Mou,[1,2,3] and Daw-Wei Wang[1,2]
[1]Department of Physics, National Tsing-Hua University, Hsinchu 30013, Taiwan, Republic of China
[2]Physics Division, National Center for Theoretical Sciences, Hsinchu 30013, Taiwan, Republic of China
[3]Institute of Physics, Academia Sinica, Nankang 115, Taiwan, Republic of China
(Received 18 December 2015; published 14 July 2016)

We examine possible low-temperature phases of a repulsively Rydberg-dressed Fermi gas in a three-dimensional free space. It is shown that the collective density excitations develop a roton minimum, which is softened at a wave vector smaller than the Fermi wave vector when the particle density is above a critical value. The mean field calculation shows that, unlike the insulating density wave states often observed in conventional condensed matters, a self-assembled metallic density wave state emerges at low temperatures. In particular, the density wave state supports a Fermi surface and a body-centered-cubic crystal order at the same time with the estimated critical temperature being about one tenth of the noninteracting Fermi energy. Our results suggest the emergence of a fermionic quantum solid that should be observable in the current experimental setup.

DOI: 10.1103/PhysRevLett.117.035301

Introduction.—It is well known that the system of repulsively interacting Fermi gases is mainly controlled by the celebrated Fermi liquid (FL) theory [1]. The breakdown of the FL theory may lead to exotic orders even without a lattice potential. For example, in the strong interaction regime, the ground state may become unstable to a nematic state by breaking the rotational symmetry via a Fermi surface distortion [Pomeranchuk instability (PI) [2]]. For systems of a long-ranged Coulomb or dipolar interaction, it is known that particles can be "frozen" locally without exchanging their positions and form a classical crystal with one particle per site in the dilute or dense limit [3–5]. In another extreme situation, such as high density ^{3}He under pressure, the ground state can be even tuned from the FL into a quantum solid [6,7], where particles self-assemble a crystal order but are still intrinsically restless and exchanging their positions even at the absolute zero of temperature.

However, in the traditional condensed matter systems, these interesting phases (nematic state, classical crystal, and quantum solid) cannot be achieved easily because the interaction strength has to be strong enough to compete with the Fermi energy. On the other hand, in the system of Rydberg atoms, the length scale and the strength of the effective interatom interaction can be manipulated easily by external fields [8–12]. In addition to the blockade effect for on-resonant excitations [13–16], one can also apply a far-detuned weak field [see Fig. 1(a)] to generate an effective Rydberg-dressed interaction (RDI), which has a soft core and a finite interaction range [see Fig. 1(b)] [17–19]. Theoretical calculations show that a repulsive RDI in a Bose gas may lead to a supersolid droplet phase [18–22], while an attractive RDI induces a 3D bright soliton [23]. For a Rydberg Fermi gas, some topological phases are also predicted for an attractive [24] or repulsive interaction in a optical lattice near half filling [25]. Recently, the RDI has been observed for two individually trapped atoms [26] and in a 2D optical lattice by measuring the spin correlation [27].

In this Letter, we demonstrate that a self-assembled metallic quantum solid phase can emerge in a single-species Fermi gas even for a *weakly* repulsive RDI in a 3D continuous space. The quantum phase transition from FL to quantum solid is driven by the interaction range of the RDI, and it is shown to be a first order transition near the collective mode softening point at a wave vector smaller than the Fermi wave vector. The new ground state, a metallic quantum solid, has a gapless fermionic excitation on top of a density wave order, which has a body-centered-cubic (bcc) structure with a lattice constant a few times larger than the averaged interparticle distance; i.e., each unit cell contains many noninteger fermionic atoms to form a Fermi sea. The critical temperature of the density wave order is estimated about $0.1E_F^0$, where E_F^0 is the noninteracting Fermi energy. Our results open a new pathway to form nonconventional correlated quantum states.

Effective interaction.—Here, we consider a single-species Fermi gas, where each atom is weakly coupled to its s-wave Rydberg state by an off-resonant two-photon transition via an intermediate state; see Fig. 1(a). In the far detuning and weak coupling limit, we can apply the standard perturbative and adiabatic approximation [18] to obtain the RDI between dressed-state atoms: $V_{\mathrm{RD}}(\mathbf{r}) = (U_0/1 + (r/R_c)^6)$ [19,23,24,28], where Ω and Δ are the effective Raman coupling and the detuning, respectively. $U_0 \equiv (\Omega/2\Delta)^4 C_6/R_c^6$, and $R_c \equiv (C_6/2|\Delta|)^{1/6}$ are the interaction strength and the averaged soft-core radius. C_6 is the averaged van der Waals coefficient, which can be shown to be positive for all orbital states when exciting

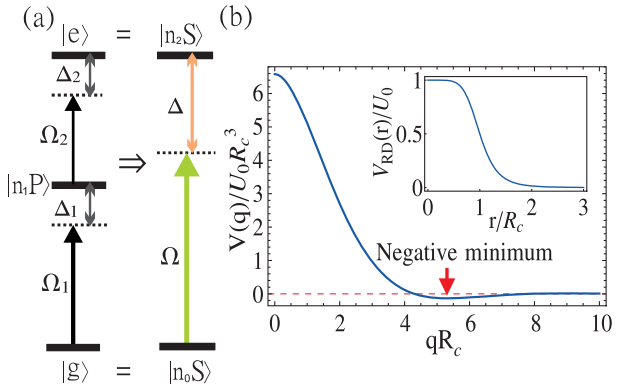

FIG. 1. (a) Schematic plot for a two-photon excitation for an off-resonant coupling between the ground state ($|n_0S\rangle$) and a Rydberg state ($|n_2S\rangle$) via an intermediate state ($|n_1P\rangle$). $\Delta_{1,2}$ and $\Omega_{1,2}$ are the detuning and Rabi frequencies, respectively. An effective single photon expression can be obtained with $\Delta = \Delta_1 + \Delta_2$ and $\Omega = \Omega_1\Omega_2/2\Delta_1$. (b) Effective Rydberg-dressed interaction in the far detuning limit ($\Delta \gg \Omega$) in the momentum space. The insert shows the corresponding real space profile with the blockade radius, R_c.

^{6}Li or ^{40}K to a state with $n > 30$ [29,30]. The decay rate of the two-photon process can be reduced by choosing a larger detuning in the first transition (say, $\Omega_1/\Delta_1 \ll 1$).

We note that the RDI discussed above is more justified for the single-species Fermi gas [24] than for bosonic systems, because the Pauli exclusion principle can strongly reduce the possible atomic loss due to the orbital level crossing in the short-distance regime. As a result, we can calculate the scattering amplitude in 3D free space (valid in the weak interaction limit, $U_0/E_F^0 \ll k_F^0 R_c$ [31]) by the first Born approximation: $V(\mathbf{q}) \equiv \int d\mathbf{r} V_{\mathrm{RD}}(\mathbf{r}) e^{-i\mathbf{q}\cdot\mathbf{r}} = U_0 R_c^3 \tilde{V}(|\mathbf{q}|R_c)$, where

$$\tilde{V}(s) = \frac{2\pi^2}{3s}\left[1 + 2e^{s/2}\sin\left(\frac{\sqrt{3}s}{2} - \frac{\pi}{6}\right)\right]e^{-s} \qquad (1)$$

is a single-parameter function with $s \equiv |\mathbf{q}|R_c$. As shown in Fig. 1(b), such a scattering amplitude has a negative minimum at a finite wave vector, $|\mathbf{q}| = Q_c \sim 5.3/R_c$. This special property results from the blockade effects of the RDI in real space [see the inset in Fig. 1(b)] and does *not* exist in other kinds of long-ranged interactions (say, Coulomb or dipolar interactions).

Collective density mode softening.—To investigate the possible density wave order, we first calculate the retarded density correlation function, $D^R(\mathbf{q},\omega) \equiv -i\int_0^\infty dt e^{-i\omega t}\langle[\rho(\mathbf{q},t),\rho(-\mathbf{q},0)]\rangle$, with the density operator $\rho(\mathbf{q}) \equiv \sum_{\mathbf{k}} c^\dagger_{\mathbf{k}+\mathbf{q}} c_{\mathbf{k}}$ ($c_{\mathbf{k}}$ is the field operator of Rydberg-dressed fermions). The density correlation function is directly related to the full polarizability, $\Pi(\mathbf{q},\omega)$ [$\mathrm{Re}D^R = \mathrm{Re}\Pi$, $\mathrm{Im}D^R = \mathrm{sgn}(\omega)\mathrm{Im}\Pi$ [32]], which can be evaluated through a Dyson series:

$$\Pi(\mathbf{q},\omega) = \frac{\Pi^*(\mathbf{q},\omega)}{1 - V(\mathbf{q})\Pi^*(\mathbf{q},\omega)}, \qquad (2)$$

with $\Pi^*(\mathbf{q},\omega)$ being the irreducible polarizability.

In our present Rydberg-dressed system, we are interested in the regime of a long blockade radius (or in the high density limit, $k_F^0 R_c \gg 1$), so that the direct energy contributes much larger than the exchange and correlation ones (similar to the case of a Coulomb interaction in the high density limit [32]). As a result, the random phase approximation (RPA) is justified; i.e., the irreducible polarizability (Π^*) can be replaced by the noninteracting polarizability, $\Pi_0(\mathbf{q},\omega) = (-i/(2\pi)^4)\int d^3k d\nu G_0(\mathbf{k},\nu)G_0(\mathbf{k}+\mathbf{q},\omega+\nu)$, where $G_0(\mathbf{k},\omega)$ is the noninteracting Green's function [32].

In Fig. 2(a), we show a typical spectral weight of the collective mode excitations within RPA. The dispersion of the collective mode is determined from the pole of $\Pi(\mathbf{q},\omega)$, i.e., $1 = V(q)\mathrm{Re}\Pi_0(q,\omega_q)$ and $\mathrm{Im}\Pi_0(q,\omega_q) = 0$ (i.e., outside the regime of particle-hole excitations [33,34]). In the long wavelength limit, this mode has a linear dispersion, $\omega_q = cq + \mathcal{O}(q^2)$, with the zero sound velocity, $c \equiv v_F^0[1 + 2e^{-2}\exp(-3/mk_F^0U_0R_c^3)]$ (v_F^0 is the noninteracting Fermi velocity). In the shorter wavelength (or larger wave vector) regime, the collective excitation

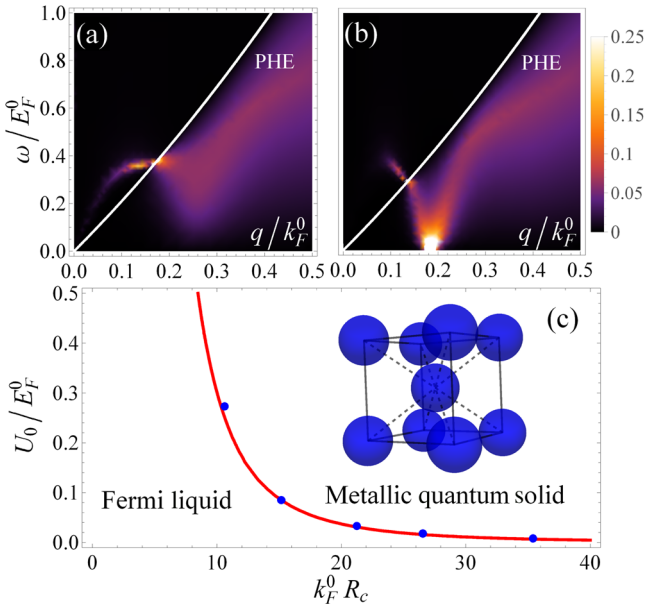

FIG. 2. Spectral weights [$\propto \mathrm{Im}\Pi(q,\omega)$] of the collective excitations with $U_0/E_F^0 = 0.012$, for (a) $k_F^0 R_c = 20$ and (b) $k_F^0 R_c = 29$, respectively. The white thin lines indicate the regime of particle-hole excitations (PHE), and the roton minimum reaches zero energy in (b). (c) Phase diagram between the FL and the metallic quantum solid. The red solid line is determined by the collective mode softening, while the blue dots are by minimizing the total mean field energy. (Inset) Schematic plot of the bcc structure.

is strongly damped and broadened by particle-hole excitations.

However, when the interaction range (R_c) is tuned larger (or in a higher density regime), we find that the roton excitation is softened at a finite momentum [$q = Q_c \sim 0.2k_F^0$, as shown in Fig. 2(b)]. In fact, since $\mathrm{Im}\Pi_0(q, \omega \to 0) \to 0$, the condition to have such roton softening can be analytically derived as $k_F^0 R_c \gg 1$:

$$\frac{U_0}{E_F^0} \times (k_F^0 R_c)^3 \geq \frac{4\pi^2}{|\tilde{V}(5.3)|} \approx 294.6. \tag{3}$$

In Fig. 2(c), we show the obtained quantum phase diagram, where Landau's FL theory fails in the high density regime ($R_c k_F^0 \gg 1$) in the 3D systems and even the interaction strength (U_0/E_F^0) is small. Note that this result follows the same condition to justify the first Born approximation and the RPA used in our theoretical calculation. Similar results can be also obtained in 1D and/or 2D systems, while the above two approximations may not be justified. We emphasize that such an interesting result does not appear in other long-ranged interactions (such as Coulomb or dipolar interactions) because the negative minimum of $V(\mathbf{q})$ originates from the sharp changes of the interaction profile due to blockade effects [see Fig. 1(b)]. We also have examined that there is no possibility of having PI within the parameter regime considered here.

Mean field approach.—Inspired by the softening of the collective excitation at a finite (but small) momentum, it is reasonable to expect a density wave order. As a result, the expectation value of the density operator in momentum space [$\equiv\rho(\mathbf{q})$] can be written $\langle\rho(\mathbf{q})\rangle = N\delta_{\mathbf{q},0} + N_1 \sum_{i=1}^{z} \delta_{\mathbf{q},\mathbf{Q}_i}$, where N is the total particle number and N_1 is the order parameter of the density wave order. $\mathbf{Q}_i$ $(i = 1, \ldots, z)$ are the wave vectors for describing the density wave order with $|\mathbf{Q}_i| = Q_{\mathrm{lat}}$. Here, we have assumed, for simplicity, that the density modulation mostly comes from the first harmonic components, and the reciprocal lattice wave vector, Q_{lat}, is a variational parameter to be determined by minimizing the total energy. For example, for a cubic lattice, we have $z = 6$ and $\mathbf{Q}_i/Q_{\mathrm{lat}} = \pm\hat{\mathbf{x}}$, $\pm\hat{\mathbf{y}}$, $\pm\hat{\mathbf{z}}$. For a face-centered-cubic (fcc) lattice in the momentum space, we have $z = 12$ and $\mathbf{Q}_1/Q_{\mathrm{lat}} = (\hat{\mathbf{x}}+\hat{\mathbf{y}})/\sqrt{2}$, $\mathbf{Q}_2/Q_{\mathrm{lat}} = (\hat{\mathbf{x}}+\hat{\mathbf{z}})/\sqrt{2}$, $\mathbf{Q}_3/Q_{\mathrm{lat}} = (\hat{\mathbf{y}}+\hat{\mathbf{z}})/\sqrt{2}$ as the three basis vectors. The other nine Q_i's can be obtained by a linear combination of $\mathbf{Q}_{1,2,3}$ and can have the same amplitude as shown in Fig. 4(a).

Following the standard mean field approximation, we replace the density operator in the Hamiltonian with its expectation value. Since there is no underlying lattice potential for fermions, we do not expect the nesting effect at any commensurate filling. After neglecting higher order fluctuations, we obtain the following effective mean field Hamiltonian:

$$H = \sum_{\mathbf{k}\in 1\mathrm{BZ}} \left[\sum_{\mathbf{n}} \varepsilon_{\mathbf{k},\mathbf{n}} c^\dagger_{\mathbf{k},\mathbf{n}} c_{\mathbf{k},\mathbf{n}} + \frac{N_1 V(Q_c)}{\Omega_v} \sum_{\langle \mathbf{n},\mathbf{n}'\rangle} c^\dagger_{\mathbf{k},\mathbf{n}'} c_{\mathbf{k},\mathbf{n}} \right] - \frac{zN_1^2}{2\Omega_v} V(Q_c), \tag{4}$$

where we have folded the whole momentum space into the first Brillouin zone (1BZ), and defined $c_{\mathbf{k},\mathbf{n}}$ to be the field operator at momentum $\mathbf{k}$, shifted by a Bravais vector, $\mathbf{K}_\mathbf{n} \equiv \sum_{i=1}^{3} n_i \mathbf{Q}_i$. Here, $\mathbf{Q}_{1,2,3}$ are the three primitive vectors in the Bravais lattice, and $\mathbf{n} \equiv (n_1, n_2, n_3)$ is an integer vector labeling the band index. $\langle \mathbf{n}, \mathbf{n}' \rangle$ denotes the two neighboring unit cells, i.e., $|\mathbf{K}_\mathbf{n} - \mathbf{K}_{\mathbf{n}'}| = Q_{\mathrm{lat}}$. Finally, $\varepsilon_{\mathbf{k},\mathbf{n}} \equiv (\mathbf{K}_\mathbf{n} + \mathbf{k})^2/2m$ denotes the noninteracting band energy, and Ω_v is the volume of the system.

The mean field Hamiltonian in Eq. (4) is then diagonalized by a unitary transformation: $\tilde{c}_{\mathbf{k},\mathbf{n}} = \sum_{\mathbf{n}'} U^*_{\mathbf{n},\mathbf{n}'}(\mathbf{k}) c_{\mathbf{k},\mathbf{n}'}$, where $\tilde{c}_{\mathbf{k},\mathbf{n}}$ is the eigenstate operator with an eigenenergy $\tilde{\varepsilon}_{\mathbf{k},\mathbf{n}}$. At zero temperature, the total energy for a given chemical potential, μ, can be obtained as $E_{\mathrm{tot}}(N_1) = \sum_{\mathbf{k},\mathbf{n}} \tilde{\varepsilon}_{\mathbf{k},\mathbf{n}} \theta(\mu - \tilde{\varepsilon}_{\mathbf{k},\mathbf{n}}) - (zN_1^2/2\Omega_v) V(Q_c)$, where $\theta(x)$ is the Heaviside function and the chemical potential (μ) is determined by the total particle number.

The order parameter, $N_1 = \sum_{\mathbf{k}} \langle c^\dagger_{\mathbf{k}+\mathbf{Q}_1} c_{\mathbf{k}} \rangle$, is then determined self-consistently from the following equation:

$$N_1 = \sum_{\mathbf{k}\in 1\mathrm{BZ}} \sum_{\mathbf{n},\mathbf{m}} U_{\mathbf{m},\mathbf{n}} U^*_{\mathbf{m},\mathbf{n}+\mathbf{e}_x} f(\tilde{\varepsilon}_{\mathbf{k},\mathbf{m}}), \tag{5}$$

where we set $\mathbf{Q}_1 = \mathbf{e}_x$ and $f(x) = (e^x + 1)^{-1}$ is the Fermi distribution function. Note that the transformation matrix element $U_{\mathbf{m},\mathbf{n}}$ depends on N_1 also.

Order parameter and band structure.—In the numerical calculation, we first consider different types of crystal order and compare their ground state energies for different values of Q_{lat}. The order parmeter, N_1, and the chemical potential are calculated self-consistently. We find that a bcc lattice [see the inset of Fig. 2(c) with the closest sphere packing fcc structure in the reciprocal lattice [35]; see Fig. 4(b)] is energetically most favorable when the density wave order is formed.

In Fig. 3, we show how the order parameter fraction, N_1/N, self-consistently calculated from Eq. (5), changes sharply from zero to a finite value as $U_0/E_F^0 \geq 0.033$ for $R_c k_F^0 = 21$. In the inset, we show how the total energy changes as a function of N_1/N near the transition point. Both results indicate that the quantum phase transition from a FL state to a density wave state is first order, consistent with earlier studies on classical liquid-solid transition [36]. The phase transition boundary is very close to the results given by roton mode softening [see Fig. 2(c)] and the obtained reciprocal lattice wave vector, Q_{lat}, is almost the same (within a 5% difference) as the one obtained by roton softening (Q_c). Results from these two independent

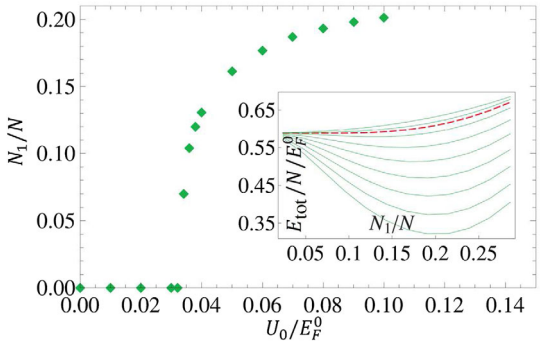

FIG. 3. The density wave order parameter, N_1/N, as a function of the interaction strength, U_0/E_F^0, for $k_F^0 R_c \sim 21$. We find that N_1/N jumps discontinuously at $U_0/E_F^0 \sim 0.033$, indicating a first order quantum phase transition. (Inset) The total energy per particle as a function of the order parameter, N_1/N, for various U_0/E_F^0's, from 0.03 (top) to 0.04 by a step 0.002, and then $U_0/E_F^0 = 0.05$, 006, and 0.07 (bottom), respectively. The red dashed line indicates the transition point, which has a local zero energy minimum at $N_1/N \sim 0.07$.

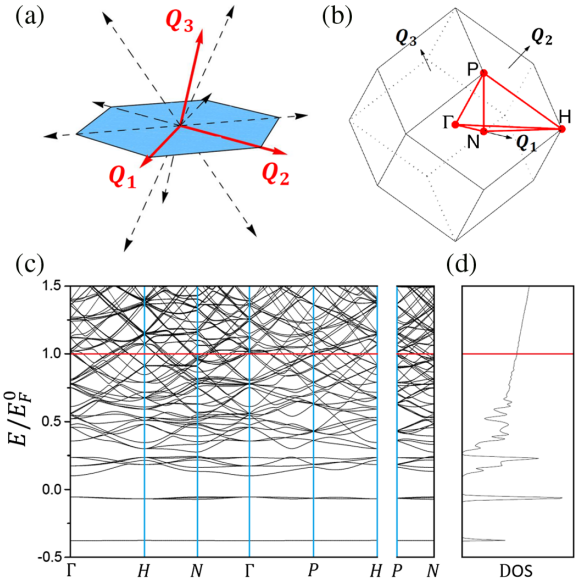

FIG. 4. (a) Twelve reciprocal vectors of the density wave with a bcc structure, pointing to the 12 reciprocal lattice points closest to the origin. The red solid arrows, $\mathbf{Q}_{1,2,3}$, denote the three basis vectors. (b) The first Brillouin zone of a bcc lattice with several high symmetry points. (c) The single particle band structure in a metallic density wave state for $R_c k_F^0 = 10.62$ and $U_0/E_F^0 = 0.28$. The horizontal red line indicates the chemical potential of noninteracting system. (d) The corresponding density of states (DOS).

approaches agree very well and hence confirm such a new quantum phase transition in a Rydberg-dressed Fermi gas. We further note that since $Q_{\rm lat} \sim Q_c \ll k_F^0$ in the parameter regime we consider here, it implies that there are many fermionic atoms in each density wave period $[\sim (k_F^0/Q_c)^3 = (21/5.3)^3 = 62.2$ in this case]. In other words, a new Fermi surface is formed in such a lattice structure, leading to a metallic density wave state.

In Fig. 4, we further show the single particle band structure [Fig. 4(c)] and the density of states [Fig. 4(d)] in the density wave phases for a typical parameter. We note that the elementary excitations near the Fermi surface are essentially gapless, while some band gaps are opened *under* the Fermi energy. These results indicate that if only the first band is occupied in the dilute limit (say, $R_c k_F^0 < 3.2$ in our calculation, while the first Born and mean field approximations may not be justified in this regime), the density wave has an effective one particle per site in the real space. Such a system is incompressible because it requires a finite energy to add one more particle inside the blockage radius, R_c [see the inset of Fig. 1(b)]. However, when adding more particles in each site, the Pauli exclusion principle starts to make fermions occupy higher bands, which have higher tunneling probability to neighboring sites and hence form a continuous band with a gapless excitation, leading to a metallic quantum solid.

We can further estimate the critical temperature of such a density wave order by solving Eq. (5) with $N_1 \to 0$, and find $T_c \sim 0.1 E_F^0$ near the phase transition boundary. This indicates that the metallic quantum solid phase proposed above can be achieved within the present experimental setup. More sophisticated calculations made by including the lattice fluctuations is beyond the scope of this Letter and will be investigated in the future.

Experimental measurement.—In a realistic experiment, one can tune the RDI in a very wide range by the external field. Taking ^{6}Li as an example, with an atomic density $n = 10^{14}$ cm^{-3}. One can choose an effective two-photon Rabi frequency $\Omega = 200$ kHz with an effective detuning $\Delta = 1$ MHz. These parameters can lead to $U_0 = 200$ Hz and $R_c = 4.1$ μm at the phase transition boundary, when choosing a Rydberg state $n = 48$ ($C_6 = 8.92$ GHz μm^6 [30]). If using ^{40}K atoms with the same density, effective Rabi frequency, and detuning, we have $U_0 = 25$ Hz and $R_c = 2.18$ μm at the phase transition boundary by coupling to the $n = 36$ state ($C_6 = 0.214$ GHz μm^6 [30]). Changing different detuning or Rydberg levels can easily change the effective interaction range or strength. Besides, we note that a similar quantum solid may also be observable if using a single photon transition to couple to a Rydberg state in a p orbital, while the obtained effective interaction might be anisotropic and lead to a different lattice order.

To reduce the loss rate in the intermediate level, which is the most dominant loss channel [18], we can use a larger detuning compared to the Rabi frequency for the first transition (i.e., $\Delta_1 \gg \Omega_1$), as shown in Fig. 1(a). Since $\gamma_1^{-1} \sim 100$ ns is the nature lifetime of the intermediate state due to the spontaneous decay, we can estimate the effective lifetime to be $\tau_{\rm eff} \sim (2\Delta_1/\Omega_1)^2 \gamma_1^{-1} \sim 0.1$ sec by choosing $\Delta_1 \sim \Delta = 1$ MHz and $\Omega_1 = 1$ kHz. Note that one can have a strong second transition—say, $\Omega_2 \sim 400$ MHz

(see Ref. [18])—to give $\Omega = \Omega_1\Omega_2/2\Delta_1 = 200\,\mathrm{kHz}$. Therefore, the effective lifetime of the system (~0.1 sec) should be long enough in the current experimental situation.

Finally, when considering a Rydberg-dressed Fermi gas trapped in a harmonic potential, one can apply the local density approximation when the cloud size is much larger than the lattice constant. Since the phase transition is first order, we expect a metallic quantum solid in the cloud center (higher density) with a discontinuous density slope near the interface with a surrounding normal cloud. Furthermore, in the long time-of-flight experiments, one can map out the Fermi surface geometry [see Fig. 4(b)] in the momentum distribution, and the density-density correlation function should also be observable through the noise correlation measurement.

Conclusion.—We find a new type of quantum phase transition of single-component fermionic atoms with a repulsive Rydberg-dressed interaction. The observed metallic density wave phase results from the softening of the collective mode excitations with a bcc structure in the 3D real space. Our results suggest the emergence of a new type of fermionic metallic quantum solid, which should be observable in future experiments.

We appreciate the fruitful discussions with T. Pohl, H.-H. Jen, and E. Demler. This work is supported by MoST and NCTS in Taiwan.

W.-H. L. and T.-C. H. contributed equally to this work.

*zihcisie@gmail.com

[1] L. D. Landau, Sov. Phys. JETP **3**, 920 (1957).
[2] J. Quintanilla and A. J. Schofield, Phys. Rev. B **74**, 115126 (2006).
[3] E. Wigner, Phys. Rev. **46**, 1002 (1934).
[4] G. Grüner, Rev. Mod. Phys. **60**, 1129 (1988).
[5] M. A. Baranov, H. Fehrmann, and M. Lewenstein, Phys. Rev. Lett. **100**, 200402 (2008).
[6] E. R. Dobbs, *Solid Helium Three* (Clarendon Press, Oxford, 1994).
[7] E. Polturak and N. Gov, Contemp. Phys. **44**, 145 (2003).
[8] Y. O. Dudin and A. Kuzmich, Science **336**, 887 (2012).
[9] U. Raitzsch, V. Bendkowsky, R. Heidemann, B. Butscher, R. Löw, and T. Pfau, Phys. Rev. Lett. **100**, 013002 (2008).
[10] J. D. Pritchard, D. Maxwell, A. Gauguet, K. J. Weatherill, M. P. A. Jones, and C. S. Adams, Phys. Rev. Lett. **105**, 193603 (2010).
[11] J. Nipper, J. B. Balewski, A. T. Krupp, B. Butscher, R. Low, and T. Pfau, Phys. Rev. Lett. **108**, 113001 (2012).
[12] P. Schauß, M. Cheneau, M. Endres, T. Fukuhara, S. Hild, A. Omran, T. Pohl, C. Gross, S. Kuhr, and I. Bloch, Nature (London) **491**, 87 (2012).
[13] D. Jaksch, J. I. Cirac, P. Zoller, S. L. Rolston, R. Côté, and M. D. Lukin, Phys. Rev. Lett. **85**, 2208 (2000).
[14] M. D. Lukin, M. Fleischhauer, R. Cote, L. M. Duan, D. Jaksch, J. I. Cirac, and P. Zoller, Phys. Rev. Lett. **87**, 037901 (2001).
[15] E. Urban, T. A. Johnson, T. Henage, L. Isenhower, D. D. Yavuz, T. G. Walker, and M. Saffman, Nat. Phys. **5**, 110 (2009).
[16] A. Gaëtan, Y. Miroshnychenko, T. Wilk, A. Chotia, M. Viteau, D. Comparat, P. Pillet, A. Browaeys, and P. Grangier, Nat. Phys. **5**, 115 (2009).
[17] J. B. Balewski, A. T. Krupp, A. Gaj, S. Hofferberth, R. Lw, and T. Pfau, New J. Phys. **16**, 063012 (2014).
[18] N. Henkel, R. Nath, and T. Pohl, Phys. Rev. Lett. **104**, 195302 (2010).
[19] N. Henkel, F. Cinti, P. Jain, G. Pupillo, and T. Pohl, Phys. Rev. Lett. **108**, 265301 (2012).
[20] H. P. Büchler, E. Demler, M. Lukin, A. Micheli, N. Prokof'ev, G. Pupillo, and P. Zoller, Phys. Rev. Lett. **98**, 060404 (2007).
[21] F. Cinti, P. Jain, M. Boninsegni, A. Micheli, P. Zoller, and G. Pupillo, Phys. Rev. Lett. **105**, 135301 (2010).
[22] G. Pupillo, A. Micheli, M. Boninsegni, I. Lesanovsky, and P. Zoller, Phys. Rev. Lett. **104**, 223002 (2010).
[23] F. Maucher, N. Henkel, M. Saffman, W. Królikowski, S. Skupin, and T. Pohl, Phys. Rev. Lett. **106**, 170401 (2011).
[24] B. Xiong, H. H. Jen, and D.-W. Wang, Phys. Rev. A **90**, 013631 (2014).
[25] X. Li and S. Das Sarma, Nat. Commun. **6**, 7137 (2015).
[26] Y.-Y. Jau, A. M. Hankin, T. Keating, I. H. Deutsch, and G. W. Biedermann, Nat. Phys. **12**, 71 (2016).
[27] J. Zeiher, R. van Bijnen, P. Schauß, S. Hild, J.-y. Choi, T. Pohl, I. Bloch, and C. Gross, arXiv:1602.06313.
[28] J. Honer, H. Weimer, T. Pfau, and H. P. Büchler, Phys. Rev. Lett. **105**, 160404 (2010).
[29] T. G. Walker and M. Saffman, Phys. Rev. A **77**, 032723 (2008).
[30] K. Singer, J. Stanojevic, M. Weidemüller, and R. Côté, J. Phys. B **38**, S295 (2005).
[31] L. D. Landau and E. M. Lifshitz, *Quantum Mechanics* (Addison-Wesley, Reading, MA, 1958), Chap. 17, Sec. 125.
[32] A. L. Fetter and J. D. Walecka, *Quantum Theory of Many-Particle Systems*, Dover Books on Physics (Dover, New York, 2003), Secs. 9, 12, and 15.
[33] G. D. Mahan, *Many-Particle Physics* (Plenum, New York, 1981), Chap. 5, Sec. 5.5.
[34] D.-W. Wang and S. Das Sarma, Phys. Rev. B **65**, 035103 (2001).
[35] N. W. Ashcroft and N. D. Mermin, *Solid State Physics* (Cengage, Boston, 1976), Chaps. 4 and 5.
[36] L. D. Landau, Phys. Z. Sowjetunion **11**, 545 (1937).